C. R. Chimie 17 (2014) 785–789

Contents lists available at ScienceDirect

Comptes Rendus Chimie

www.sciencedirect.com

Full paper/Mémoire

Comparative study of the catalytic hydroconversion of cyclopentane over iridium and platinum single-crystal surfaces☆

Franck Morfin, Salim Nassreddine, Laurent Piccolo *

Institut de recherches sur la catalyse et l'environnement de Lyon (IRCELYON), UMR 5256 CNRS, Université Lyon-1, 2, avenue Albert-Einstein, 69626 Villeurbanne cedex, France

ARTICLE INFO

Article history:
Received 19 July 2013
Accepted after revision 28 October 2013
Available online 17 May 2014

Keywords:
Heterogeneous catalysis
Cyclopentane
Ring opening
Dehydrogenation
Iridium
Platinum
Single crystals

ABSTRACT

In the context of fuel upgrading by selective ring opening of naphthenes, we have investigated the catalytic conversion of cyclopentane in large hydrogen excess over iridium and platinum single-crystal surfaces. Both (111) and (112) orientations have been considered. The catalytic tests have been performed at 1 kPa and 25–600 °C using a recently developed surface reactor equipped with laser heating and online gas chromatography. Only cyclopentene and C_1–C_4 cracking products are formed on iridium, while platinum additionally catalyzes the formation of pentane around 200 °C, which dehydrogenates to pentene at 250 °C. Noticeably, on both metals, the surface steps prevent hydrocarbon cracking (up to 400 °C) at the benefit of dehydrogenation. In all cases, a carbon overlayer is formed on the surfaces in the course of the reaction.

1. Introduction

Depending on the catalytic conditions, a paraffin (open-chain alkane) or a naphthene (cyclo-alkane) interacting with a platinum-group metal can undergo various transformations, including dehydrogenation, isomerization, and hydrogenolysis [1,2]. Hydrogenolysis of a naphthenic ring may lead to ring opening (breaking of one C–C bond) or cracking (breaking of several C–C bonds). The selective ring opening (SRO) process consists ideally of the conversion or aromatic and naphthenic hydrocarbons into linear paraffins with an unchanged number of C atoms [3]. It is currently the subject of intense research due to the envisioned shortening of conventional energy sources. Indeed, in combination with aromatics saturation, this process is expected to improve the cetane number (CN) of highly aromatic and hardly exploited petroleum cuts, such as the light cycle oil. However, catalytic SRO is still far from being efficient due to the difficulty in opening rings selectively, i.e., at substituted carbon positions in order to avoid the formation of branched paraffins, which have lower CNs than the linear ones [4]. Current research in SRO focuses on the use of oxide–metal bifunctional catalysts [5–11], although some attempts with oxide–oxide [12,13], oxide–sulfide [14,15] and oxide–carbide [16,17] combinations have also been reported. The metal nanoparticles, typically platinum or iridium, catalyze the saturation of aromatics and the hydrogenolysis of saturated C–C bonds. The additional use of oxide supports exhibiting Brønsted acidity, like zeolites or mesoporous aluminosilicates seems necessary to both provide sulfur-resistance to the metal nanoparticles and to accelerate C–C bond scission. Nevertheless, it also favors isomerization (especially ring contraction from C_6 to C_5) and cracking to undesired light products [18]. We have recently shown that the hydrogenolytic role of the metal in bifunctional catalysts

☆ Thematic issue dedicated to François Garin.

* Corresponding author.
E-mail address: laurent.piccolo@ircelyon.univ-lyon1.fr (L. Piccolo).

1631-0748/$ – see front matter
http://dx.doi.org/10.1016/j.crci.2013.10.015

is reduced due to the predominance of competitive acid-catalyzed isomerization [19]. However, metal-catalyzed hydrogenolysis appears as the only way to selectively open C–C bonds. Hence, we believe that non-acidic catalysts containing one or several noble metals must be reevaluated to address the SRO challenge.

While platinum is the reference metal in hydrogenation catalysis, iridium is known for its hydrogenolysis properties [20–24]. The use of well-defined single-crystal surfaces is the best way to compare the intrinsic catalytic properties of different metals, since there is no contribution of side effects, such as particle size, morphology, and support [25]. However, unlike for supported catalysts, to our knowledge and except for highly instable (methyl)cyclopropane [26], there has been no experimental work published on hydrocarbon ring conversion over well-defined Ir surfaces under non-UHV conditions. On Pt single-crystal surfaces, Somorjai et al. have investigated (methyl)cyclohexene hydrogenation and dehydrogenation and benzene hydrogenation [27–30]. Recently, theoretical studies of cyclic hydrocarbon adsorption and ring opening on Pt-group metal surfaces have appeared in the literature [31–33].

In this work, we have compared platinum and iridium model surfaces in the hydroconversion of cyclopentane. This molecule is both one of the simplest naphthenic compounds and an important product subunit in real hydrotreated fuels.

2. Experimental

The experimental setup used for this study has been described in details elsewhere [34]. It is briefly described below and depicted in Fig. 1. A double ultrahigh-vacuum (UHV) chamber (Fig. 1a) allows preparing the samples and analyzing them by Auger electron spectroscopy (AES) and low-energy electron diffraction (LEED). The cleaned samples can be transferred under UHV in two steps from the preparation chamber into an isolatable UHV-compatible reaction cell (Fig. 1c) of small volume (*ca.* 120 cm^3). The combination of a focused infrared laser beam and an infrared pyrometer allows one to accurately control the sample temperature from outside the cell, through portholes, without heating/outgassing the reactor walls. The reactant mixture is prepared in a dedicated chamber (Fig. 1b), and then introduced in the cell. The reactive mixture can be continuously sampled through a leak valve and analyzed by a mass spectrometer located in a separate UHV chamber. However, for this study involving a number of hydrocarbon molecules, a second gas detection system has been recently implemented on the apparatus.

The gas sampling device (Fig. 1d) includes a series of automated valves with pneumatic actuators, and is evacuated by a dry scroll pump. With this device, a fixed amount of gas is periodically sampled from the reactor and injected into the column of a gas chromatograph equipped with a flame ionization detector (GC-FID, Agilent 6850).

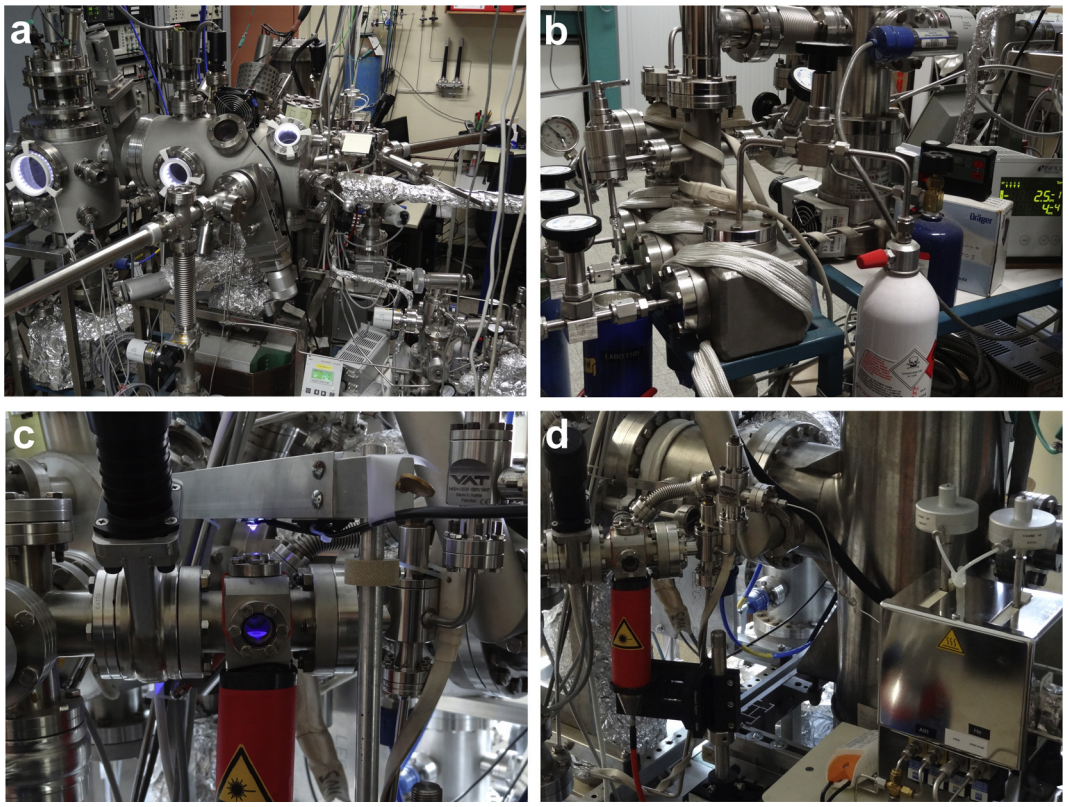

Fig. 1. (Color online.) Pictures of the experimental setup. a: general view of the UHV chambers. The reactor is at the rear, right-hand side; b: gas handling system; c: catalytic cell with IR laser and UV diode. The diode can be replaced with a pyrometer head; d: gas sampling systems for MS and GC analyses.

This original system does not require gas recirculation and balance inert gas as in conventional systems, so that low working pressures (down to *ca.* 1 Torr[1]) are permitted, which reduces the amount of impurities possibly introduced in the reactor. Moreover, the system has a high sensitivity since partial pressures smaller than 10^{-4} Torr can be detected.

In this work, the GC column was an Agilent HP-AL/KCl (50 m × 0.53 × 15 μm) and the GC method parameters optimized for the analyses were: column flow rate of 9 mL min^{-1}, split ratio of 2, constant column temperature of 100 °C. The catalyst exposed to the reactive mixture was heated from RT to 600 °C by steps of 50 or 100 °C, using at each step a 20 min plateau ending with GC sampling.

In order to determine the retention times, GC standards were injected in liquid form (1 μL) with a syringe through a septum into the injection chamber, which is connected to the sampling system and allows flash vaporization of the liquid. The retention times were determined following this procedure for all the cyclopentane hydroconversion products.

Hydrogen and argon (purchased from Air Liquide, Alphagaz 2 standard) were used without further purification. Ar serves as an internal standard. Liquid cyclopentane (Fluka, purity > 99.5%) was poured in a glass tube connected to the gas mixer via a glass–metal welding and an UHV-type regulation valve. The liquid was purified by LN_2 freeze/pump/thaw cycles.

High-purity Pt and Ir single crystals were purchased from Mateck GmbH (Germany). They were small disks of diameter 10 mm and thickness mm. They were grown, oriented (within 0.1°) and surface-polished (roughness < 30 nm) by the provider. The samples were fixed on molybdenum sample holders. The surfaces were prepared by repeated cycles of Ar^+ sputtering and annealing at 700–800 °C under UHV until no impurities could be detected by AES (see below, Fig. 5), and sharp diffraction patterns were obtained by LEED [25].

3. Results and discussion

In this study, we have compared Ir and Pt in cyclopentane hydroconversion at increasing temperatures and a total initial pressure of 12 Torr (C_5H_{10}:H_2:Ar = 1:10:1 Torr), i.e., 1.6 kPa. For each metal, the flat close-packed (111) surface has been compared to the (112) surface, which is vicinal to the (111) and consists of an alternation of <112>-oriented steps and small (111) terraces (Fig. 2).

Prior to the catalytic tests, an evaluation of the equilibrium concentrations of C_5 derivatives of cyclopentane was performed using HSC Chemistry 7 software at various temperatures for our partial pressure conditions. As shown in Fig. 3, pentane (ring opening product) is thermodynamically favored below *ca.* 350 °C, while cyclopentene (dehydrogenation product) is favored above this temperature. The equilibrium concentration of pentene is always small.

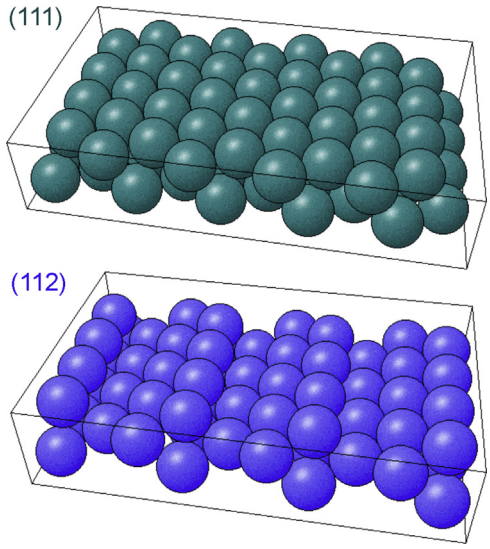

Fig. 2. (Color online.) Schematic representation of the atomic structure of (111) and (112) surfaces.
From Surface Explorer online program (http://surfexp.fhi-berlin.mpg.de/).

Fig. 4 shows the product yields for cyclopentane hydroconversion over Pt and Ir surfaces. The yield of product *i* (Y_i) is defined by: $Y_i(t) = A_i(t)/A_{CP}(t = 0)$, where A_i and A_{CP} are the areas of the GC peaks corresponding to product *i* and cyclopentane, respectively. As a matter of fact, using FID detection, the area of a GC peak is roughly proportional to the number of carbon atoms N_C^i in the corresponding hydrocarbon *i*, if the latter contains no heteroatom (here $N_C^i = 5$) [35]. Most of the yields increase with temperature. The maximum conversion reached, i.e. the sum of the yields, is below 3%.[2] Overall, the stepped surfaces are more active than the flat ones, especially for Ir at high temperatures. Surprisingly, on Ir surfaces, only cyclopentane dehydrogenation to cyclopentene and hydrocarbon cracking to smaller alkanes (C_1–C_4) take place. On Pt surfaces, *n*-pentane and *n*-pentene additionally form around 200 °C. Three pentene isomers, namely 1-pentene, *cis*-2-pentene and *trans*-2-pentene, were detected (they are grouped together in Fig. 4 for the sake of clarity). Neither branched pentane and pentene, nor pentadiene are formed. Besides, trace amounts of cyclopentadiene were detected, but only between 400 and 500 °C (not shown). As expected from thermodynamics (Fig. 3), pentane and cyclopentene are the most abundant products for Pt surfaces at low and high temperatures, respectively. The selectivity of Pt to pentane, which is the

[1] The Torr unit is the most commonly used in surface science (1 Torr = 133 Pa).

[2] From a technical viewpoint, this allows working under quasi steady-state conditions (hydrogen and cyclopentane-rich mixture) although the reactor operates in static mode. It must be kept in mind that in this working mode involving a temperature rise, a constant product yield implies that this product is no longer formed, i.e., cumulative yields are reported.

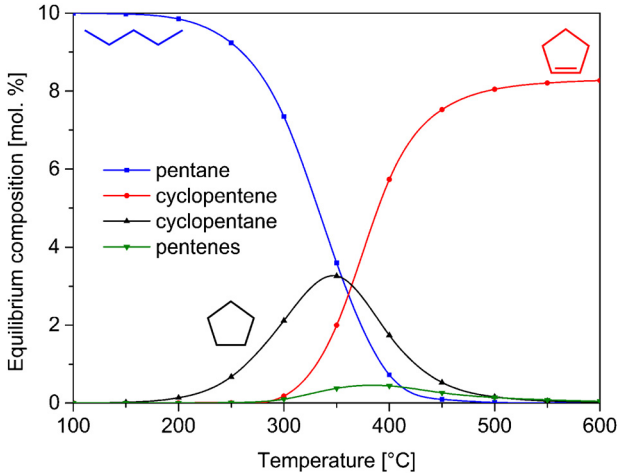

Fig. 3. (Color online.) Simulated equilibrium concentration of a gas mixture containing hydrogen (starting value 10 Torr), cyclopentane (starting value 1 Torr), cyclopentene, pentane, and pentene isomers at variable temperature.

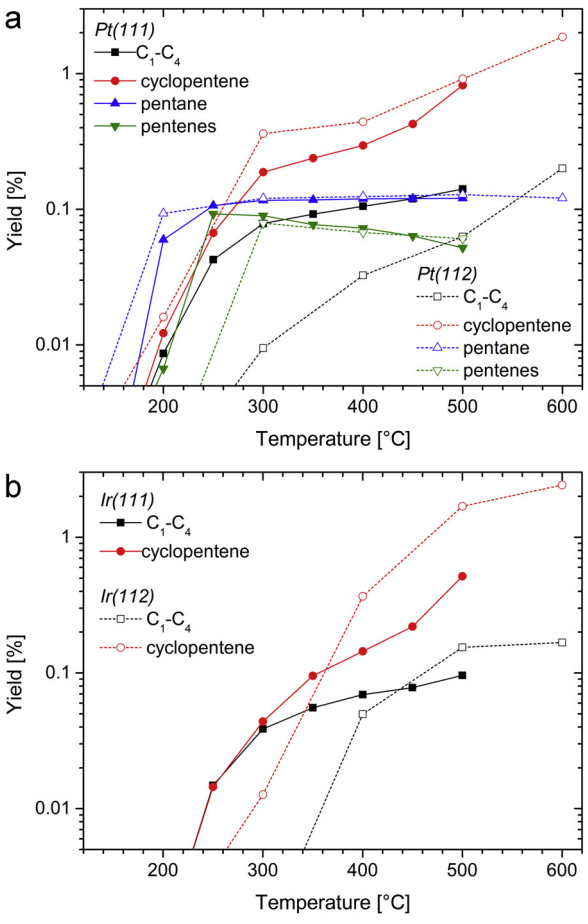

Fig. 4. (Color online.) Thermal evolution of the yields of the products formed during cyclopentane hydroconversion over Pt (a) and Ir (b) surfaces. The temperature was increased step by step, keeping a 20 min plateau at each step. Initial pressure conditions: 1 Torr C_5H_{10}, 10 Torr H_2. For Pt, the three pentene isomers have been gathered together (GC areas summed) to improve readability.

most interesting product in terms of SRO, is 70–85% around 200 °C, but it vanishes above this temperature.

Comparing Ir and Pt, in addition to the absence of ring opening products for Ir, the major difference is seen for (111) surfaces on dehydrogenation activity: depending on the temperature, Pt is 2–3 times more active than Ir. On both metals, the steps favor dehydrogenation at the expense of cracking, consistently with results for cyclohexane on Pt surfaces [23]. Indeed, light products appear at *ca.* 250 °C for (111) surfaces, whereas they are seen only above 400 °C for the (112) surfaces.

After the reaction experiments, all the surfaces were covered by a carbon layer, as attested by AES spectra (Fig. 5). Nevertheless, the model catalysts are never fully deactivated, as deduced from the product yields still increasing at the highest temperatures. Such irreversible carbon deposition has also been observed by others after hydroconversion of cyclohexane over Pt [23] and cyclopropane over Ir [26]. This process is expected to be concomitant with the formation of cracking products, since cracking is of the

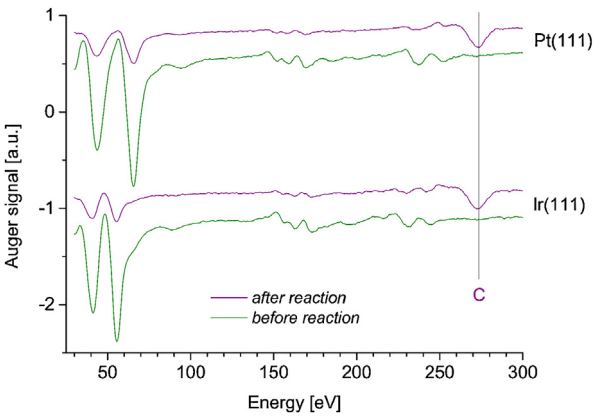

Fig. 5. (Color online.) Auger electron spectra for Pt(111) and Ir(111), before and after the catalytic tests.

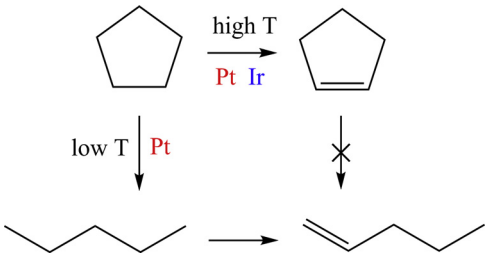

Fig. 6. (Color online.) Simplified mechanistic scheme for cyclopentane hydroconversion on Pt and Ir. Cracking steps and 2-pentene isomers are not represented.

same nature as ring opening, but it probably results from stronger adsorption of the parent species. Due to stronger adsorption of the reaction intermediates on Ir with respect to Pt [33], they must be readily hydrogenolyzed to light products and layer-forming carbonaceous adsorbates on Ir. This may explain the absence of pentane and pentene desorption from Ir and the apparent contradiction between our results for single-crystal surfaces and those of Bétizeau et al. [22], who have found a clear superiority of Ir over Pt in cyclopentane hydrogenolysis, for alumina-supported catalysts. The differences between single crystals and supported catalysts in terms of selective ring opening activity could originate from the presence, at the surface of the metal nanoparticles, of low-coordination sites which may inhibit multiple C–C bond breaking at the benefit of single bond scission.

Besides, for Pt, the appearance of pentene at *ca.* 250 °C follows that of pentane at *ca.* 200 °C and has no correlation with the behavior of cyclopentene. Thus, pentene is likely to be formed from pentane dehydrogenation, not from cyclopentene ring opening. Consistently, both pentane and pentene are not formed on Ir. Moreover, the decrease of the pentene yields along with the unchanged pentane yields suggest that, unlike pentane, pentene decomposes on the surface as the temperature increases. From the above results, the mechanistic scheme of Fig. 6 is proposed for cyclopentane conversion on Pt and Ir surfaces in the presence of excess hydrogen.

4. Conclusion

Unlike iridium surfaces, platinum surfaces are highly selective to the ring opening of cyclopentane to pentane at *ca.* 200 °C, which is most probably followed by pentane dehydrogenation to pentene at higher temperature. Both platinum and iridium mainly catalyze cyclopentane dehydrogenation above 250–300 °C. Hydrocarbon cracking (i.e., multiple C–C bond breaking) competes with the other steps and leads to the formation of carbon overlayers. However, the (112) stepped surfaces are much more resistant to hydrocarbon cracking than the (111) flat ones.

In conclusion, this surface-science study provides the first direct comparison of the intrinsic naphthene hydrogenolysis properties of iridium and platinum. Unexpectedly, platinum appears more suitable for catalyzing the single opening of C_5 naphthenes than iridium.

Acknowledgements

L.P. thanks François Garin for his inspiring works on hydrocarbons and his constant friendliness. L.P. also thanks Christophe Geantet for stimulating the SRO research. Gilles d'Orazio is acknowledged for technical assistance. The French government is acknowledged for financial support via the ANR-10-BLAN-1012 Surf-Fer project.

References

[1] F. Garin, F.G. Gault, J. Am. Chem. Soc. 97 (1975) 4466.
[2] F.G. Gault, Adv. Catal. 30 (1981) 1.
[3] G.B. McVicker, M. Daage, M.S. Touvelle, C.W. Hudson, D.P. Klein, W.C. Baird, B.R. Cook, J.G. Chen, S. Hantzer, D.E.W. Vaughan, E.S. Ellis, O.C. Feeley, J. Catal. 210 (2002) 137.
[4] R.C. Santana, P.T. Do, M. Santikunaporn, W.E. Alvarez, J.D. Taylor, E.L. Sughrue, D.E. Resasco, Fuel 85 (2006) 643.
[5] H. Du, C. Fairbridge, H. Yang, Z. Ring, Appl. Catal. A 294 (2005) 1.
[6] A. Infantes-Molina, J. Mérida-Robles, E. Rodríguez-Castellón, J.L.G. Fierro, A. Jiménez-López, Appl. Catal. B 73 (2007) 180.
[7] K.C. Mouli, V. Sundaramurthy, A.K. Dalai, Z. Ring, Appl. Catal. A 321 (2007) 17.
[8] D. Kubička, M. Kangas, N. Kumar, M. Tiitta, M. Lindblad, D.Y. Murzin, Top. Catal. 53 (2010) 1438.
[9] S. Nassreddine, L. Massin, M. Aouine, C. Geantet, L. Piccolo, J. Catal. 278 (2011) 253.
[10] V. Calemma, M. Ferrari, S. Rabl, J. Weitkamp, Fuel 111 (2013) 763.
[11] R. Moraes, K. Thomas, S. Thomas, S. Van Donk, G. Grasso, J.-P. Gilson, M. Houalla, J. Catal. 299 (2013) 30.
[12] A. Boulaoued, I. Fechete, B. Donnio, M. Bernard, P. Turek, F. Garin, Micropor. Mesopor. Mater. 155 (2012) 131.
[13] S. Haddoum, I. Fechete, B. Donnio, F. Garin, D. Lutic, C.E. Chitour, Catal. Commun. 27 (2012) 141.
[14] K. Sato, Y. Iwata, T. Yoneda, A. Nishijima, Y. Miki, H. Shimada, Catal. Today 45 (1998) 367.
[15] D. Eliche-Quesada, J. Mérida-Robles, P. Maireles-Torres, E. Rodríguez-Castellón, A. Jiménez-López, Appl. Catal. A 262 (2004) 111.
[16] X. Liu, K.J. Smith, Appl. Catal. A 335 (2008) 230.
[17] K.C. Mouli, V. Sundaramurthy, A.K. Dalai, J. Mol. Catal. A 304 (2009) 77.
[18] S. Nassreddine, S. Casu, J.L. Zotin, C. Geantet, L. Piccolo, Catal. Sci. Technol. 1 (2011) 408.
[19] L. Piccolo, S. Nassreddine, G. Toussaint, C. Geantet, ChemSusChem 5 (2012) 1717.
[20] J.H. Sinfelt, D.J.C. Yates, J. Catal. 8 (1967) 82.
[21] J.L. Carter, J.A. Cusumano, J.H. Sinfelt, J. Catal. 20 (1971) 223.
[22] C. Bétizeau, G. Leclercq, R. Maurel, C. Bolivar, H. Charcosset, R. Fréty, L. Tournayan, J. Catal. 45 (1976) 179.
[23] R.K. Herz, W.D. Gillespie, E.E. Petersen, G.A. Somorjai, J. Catal. 67 (1981) 371.
[24] A. Djeddi, I. Fechete, F. Garin, Appl. Catal. A 413–414 (2012) 340.
[25] L. Piccolo, S. Nassreddine, F. Morfin, Catal. Today 189 (2012) 42.
[26] J.R. Engstrom, D.W. Goodman, W.H. Weinberg, J. Phys. Chem. 94 (1990) 396.
[27] S.M. Davis, G.A. Somorjai, J. Catal. 65 (1980) 78.
[28] K.M. Bratlie, L.D. Flores, G.A. Somorjai, Surf. Sci. 599 (2005) 93.
[29] M. Yang, R.M. Rioux, G.A. Somorjai, J. Catal. 237 (2006) 255.
[30] K.M. Bratlie, M.O. Montano, L.D. Flores, M. Paajanen, G.A. Somorjai, J. Am. Chem. Soc. 128 (2006) 12810.
[31] X. Li, M.S.M. Wong, K.H. Lim, Theor. Chem. Acc. 127 (2010) 401.
[32] Z.-J. Zhao, L.V. Moskaleva, N. Rösch, J. Catal. 285 (2012) 124.
[33] Z.-J. Zhao, L.V. Moskaleva, N. Rösch, ACS Catal. 3 (2013) 196.
[34] F. Morfin, L. Piccolo, Rev. Sci. Instrum. 84 (2013) 094101.
[35] T. Holm, J. Chromatogr. A 842 (1999) 221.